

Long-lived near-infrared photoinduced absorption in LaSrAlO₄ excited with visible light

J. Demsar,^{1,5} A. Gozar,² V. K. Thorsmølle,^{3,4} A. J. Taylor,³ and I. Bozovic²

¹*Jozef Stefan Institute, Jamova 39, SI-1000 Ljubljana, Slovenia*

²*Brookhaven National Laboratory, Upton, New York 11973, USA*

³*Los Alamos National Laboratory, Los Alamos, New Mexico 87545, USA*

⁴*École Polytechnique Fédérale de Lausanne, CH-1015 Lausanne, Switzerland*

⁵*Department of Physics, University of Konstanz, D-78457 Konstanz, Germany*

(Received 9 July 2007; published 16 August 2007)

Here, we report on studies of photoinduced carrier dynamics in LaSrAlO₄. In samples annealed in a reductive atmosphere, intense illumination by sub-band-gap photons results in strong photoinduced absorption (PIA) centered at about 0.7 eV. As a function of temperature, PIA disappears above 200 K, but at 4 K, it has a lifetime of several hours. The nonlinear dependence of PIA on light fluence enables “writing” or “erasing” this optical memory effect by using visible and infrared photons, respectively. Our results can be explained within a three-level scheme and are discussed in a scenario that involves trapping of photoexcited electrons at oxygen-vacancy sites.

DOI: [10.1103/PhysRevB.76.054304](https://doi.org/10.1103/PhysRevB.76.054304)

PACS number(s): 78.30.-j, 78.40.-q, 78.20.-e

I. INTRODUCTION

Lanthanum strontium aluminate, LaSrAlO₄ (LSAO), is an interesting material from several points of view. It crystallizes¹ in a perovskitelike phase with the space group D_{4h}^{17} and has the same tetragonal structure (the so-called T or K₂NiF₄ structure) as the prototype high- T_c superconductor La_{2-x}Sr_xCuO₄. A good lattice match to superconducting cuprates and low dielectric loss in far-infrared and microwave ranges² make LSAO the preferred substrate for epitaxial growth of high- T_c films.³ Moreover, laser action in the infrared (IR) has been observed in Nd-doped LSAO,⁴ thus opening prospects for development of an all-solid-state laser.

The main motivation for studying IR properties of pure LSAO stems, however, from a different perspective: mid- and near-IR absorption bands centered around 0.5–0.9 eV are almost ubiquitous features in oxide materials ranging from strong dielectrics^{5,6} and magnetic compounds⁷ to high- T_c superconductors.⁸ For almost all systems, the origin of these features is still a matter of debate. Consequently, an important open question is whether the origin of these bands lies in intrinsic properties of the crystals (e.g., small polaron formation) or they are associated with extrinsic lattice defects such as oxygen vacancies.⁹

In this paper, we report on long-lived near-IR (NIR) photoinduced absorption (PIA) in LSAO excited with visible light, well below its band gap of about 5 eV.^{1,10,11} The photoinduced excitations are extremely long lived at low temperatures (T) but are wiped out by $T \approx 200$ K. The nonlinear dependence of PIA on excitation and NIR probe intensities can be described within a simple three-level scheme. The data at $T=4$ K allow for a very good description of the PIA spectral shape using the standard small polaron theory. However, we also show that PIA can be induced in “colorless” crystals by reductive annealing. This implies a complex origin of this optical memory effect involving both phonons and oxygen (O) vacancies. Given the stability of the LSAO crystals, our results imply that point defects could play a generic role in the IR carrier dynamics and that optical data

alone do not prove intrinsic polaron formation in layered oxides.

II. EXPERIMENT

A series of (100) oriented LSAO single crystals grown by the Czochralski method has been studied, some of which were postannealed in a reducing atmosphere (high vacuum or flowing argon gas). Experiments were performed in three different experimental configurations in Los Alamos and in Brookhaven. In setup *A*, the sample was excited by a frequency-doubled Nd:YVO₄ solid-state laser with a photon energy of 2.33 eV (532 nm), while PIA spectrum was measured using a Bruker IFS 66v Fourier transform infrared (FTIR) spectrometer. In setup *B*, the sample was excited by a Hg arc lamp equipped with a 2.0–3.5 eV blue bandpass filter, and PIA was recorded using a Nicolet 670 FTIR spectrometer. In setup *C*, the sample was excited by a frequency-doubled Ti:sapphire laser at 3.1 eV and probed using an optical parametric amplifier in the 0.6–2.5 eV range. The excitation fluence (I) and the IR probe intensity (P) were varied by as much as 5 orders of magnitude. In each of the three setups, LSAO crystals were placed in a continuous flow optical cryostat and T was varied between 4 and 300 K. The magnitude of PIA is determined from the relative changes in sample transmission, $-\Delta T/T$.

A. Photoinduced absorption at 0.7 eV: Origin and spectral shape

Figure 1 shows the main experimental observation: LSAO crystals excited using visible light display a dramatic suppression of transmission in the NIR range. The PIA spectrum is peaked near 0.7 eV, with a spectral width of about 0.5 eV. Various 0.5 and 1.0 mm thick LSAO crystals from different sources were studied. The magnitude of the effect was found to vary from sample to sample. The variations in magnitude of PIA can be traced to variations in the (growth-dependent) absorption coefficient in the broad absorption band above

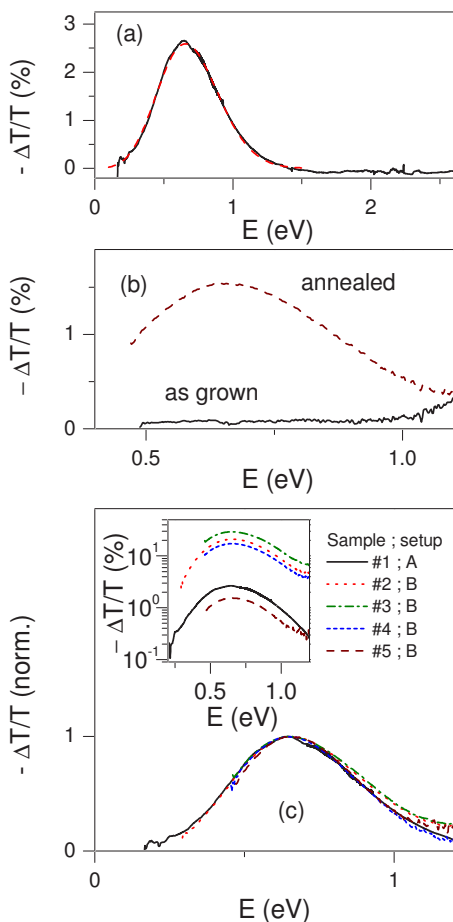


FIG. 1. (Color online) (a) The spectral shape of PIA in LSAO sample 1 recorded using setup A. It can be well fitted by the Poisson-distribution-like formula (Ref. 16) (dashed line). (b) PIA in an annealed LSAO crystal (sample 5) compared to an as-grown crystal. (c) PIA measured on five different samples (1–5) in setups A ($I=5$ W/cm² and $P=35$ mW/cm², spectrally integrated) and B ($I=0.1$ W/cm² and $P=1.7$ mW/cm², spectrally integrated). In the main panel, the data were normalized to its maximum value, while the inset shows the bare data. All data presented in this figure were recorded at 4 K.

2.5 eV, which are most likely associated with point defects due to O deficiency.^{1,11} However, as Fig. 1(c) shows, the shape of PIA remains the same in all measured crystals. Moreover, it is also identical to the spectra acquired from high quality as-grown crystals that displayed no trace of PIA after they were annealed in a reducing atmosphere (4% H + Ar). This is a robust, reproducible, and controllable effect which is directly correlated to O vacancies. We should also note that the spectral shape can be fitted perfectly by a Poisson-distribution-like formula,¹⁶ $\sigma_1(\omega) \propto e^{-\eta} (\omega_0/\omega)^{\omega/\omega_0+3/2} e^{\omega/\omega_0} \eta^{\omega/\omega_0}$, which is the standard formula for optical absorption due to electrons (or holes) self-trapped by strong coupling to optical phonons.^{15,16} The best fit is obtained with $\hbar\omega_0 \approx 70$ meV and a mean number of quanta $\eta \approx 10$.

Figure 1 clearly shows that the effect discussed here is identical in all studied LSAO samples. We also show in the

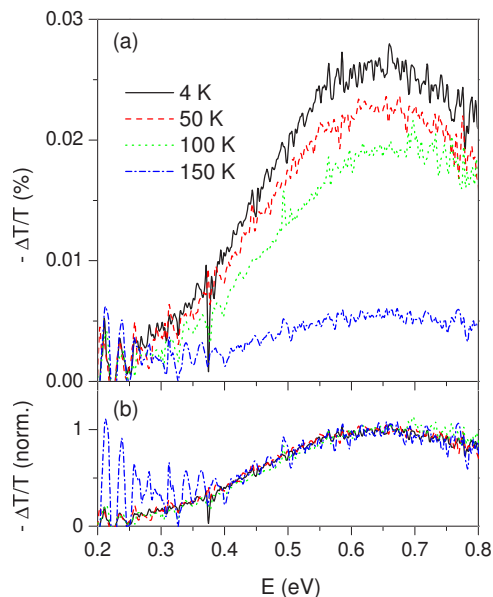


FIG. 2. (Color online) (a) The temperature dependence of the photoinduced absorption spectrum in the mid-infrared range recorded on sample 1 using setup A. (b) The data from panel (a) normalized to the peak in the PIA showing that the spectral shape does not change with temperature. This implies that the spectral shape of the PIA is independent of sample, excitation intensity, NIR probe intensity (see Fig. 1), and temperature.

following that PIA intensity depends on P , I , and T . The recovery and saturation dynamics, i.e., the time dependence of PIA after the pump light is switched off or on, are also functions of these parameters. However, no changes in the spectral shape were observed.

Figure 2 shows the recorded PIA spectrum taken at several temperatures. Apart from changes in the PIA amplitude, no measurable change in the spectral shape was detected. This allows probing PIA dynamics at its maximum value of about 0.7 eV. Accordingly, unless otherwise stated, the data shown in Figs. 3–6 were recorded using setup C with a 1 s time resolution from a representative sample (sample 1 where a change in transmission of over 33% at 0.7 eV was observed in configuration C). The maximum change in transmission of over 70% at 0.7 eV was observed in sample 3 in configuration C corresponding to the PIA coefficient $\alpha_{PI}(0.7 \text{ eV}) \approx 24 \text{ cm}^{-1}$.

B. Low temperature dynamics of the photoinduced absorption

Figure 3(a) shows the dependence of $-\Delta T/T$ recovery at 4 K as a function of P spanning over 4 orders in magnitude. The strong P dependence of the recovery and its quasiequilibrium value (when both the visible excitation I and NIR probe beam P are incident on the sample) implies that NIR quenching is the dominant term governing the relaxation and that the intrinsic relaxation limit is not reached even at the lowest probe fluence. The nearly perfect scaling obtained in Fig. 3(b) proves indeed that the relaxation is entirely governed by NIR quenching: the data from panel (a) collapse onto one another if the time axis of the individual traces is

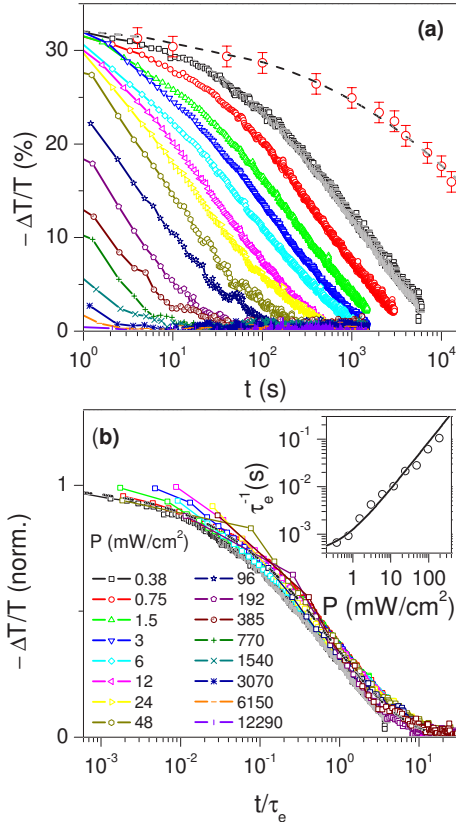


FIG. 3. (Color online) (a) Evolution of PIA at 0.7 eV with time, after the photoexcitation was switched off, as a function of P ($I = 20 \text{ W/cm}^2$ and $T = 10 \text{ K}$). The open circles denote data recorded in setup B ($P = 1.7 \text{ mW/cm}^2$) with NIR probe blocked between successive data points. (b) Scaling of the traces from panel (a), together with the fit by $A \exp[-(t/\tau_e)^p]$ with $p \sim 0.5$ (dashed line). Inset presents $\tau_e^{-1}(P)$ fit by $\tau_e^{-1} = b + dP$ (line) with $b = 0.0004 \text{ s}^{-1}$ and $d = 0.0211 \text{ s}^{-1} \text{ mW}^{-1} \text{ cm}^2$.

scaled with P and the amplitude normalized to its quasiequilibrium value. In order to determine the lower limit of intrinsic relaxation rate, PIA was recorded at different times after photoexcitation was switched off while keeping the NIR beam blocked otherwise [open symbols in Fig. 3(a)]. It follows that the intrinsic lifetime of PIA in LSAO exceeds 5 h. The decay dynamics (both the one governed by NIR quenching as well as the intrinsic one) can be represented as neither exponential nor bimolecular relaxation but can be well fitted by a phenomenological stretched exponential decay function $A \exp[-(t/\tau_e)^p]$, with the effective relaxation rate τ_e^{-1} and the stretching parameter $p \sim 0.5$ [dashed lines in panels (a) and (b)]. This suggests that the intrinsic relaxation is governed by a broad distribution of relaxation rates spanning 1 order of magnitude.¹²

At low temperatures and low photoexcitation intensities, the buildup of the PIA can also be recorded using setup C. Figure 4(a) shows the appearance of the PIA recorded on sample 1 using setup C. The PIA buildup time after photoexcitation is switched on is inversely proportional to I , showing that prior to saturation, it is dose dependent [see Fig. 4(b)].

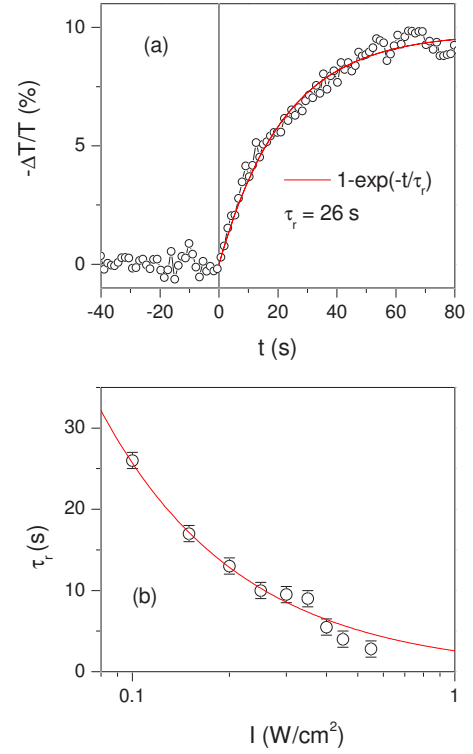


FIG. 4. (Color online) (a) The appearance of PIA after photoexcitation was switched on ($I = 100 \text{ mW/cm}^2$, $P = 3 \text{ mW/cm}^2$). Solid line is a fit to a simple saturation model $\Delta T/T \propto [1 - \exp(-t/\tau_r)]$, with $\tau_r = 26 \text{ s}$. (b) The dependence of τ_r on the photoexcitation density I . The solid line is the fit with $\tau_r \propto I^{-1}$, implying that prior to saturation PIA is dose dependent.

We assume that PIA is proportional to the concentration of in-gap excitations n_M , viz., $-\Delta T/T \propto n_M$. From the measured $\Delta T/T$, we can get a rough estimate of the density of photoinduced (PI) carriers giving rise to PIA. The PI change in optical conductivity is $\sigma_1^{PI}(\omega) = \frac{\alpha_{PI}(\omega)nc}{4\pi}$, where n is the refractive index and c the speed of light. From the partial sum rule $\int_0^\infty \sigma_1^{PI}(\omega) d\omega = \frac{\pi n_M e^2}{2m}$, we determine the density of photo-generated in-gap carriers n_M . Integrating the induced optical conductivity up to 2.5 eV, with $n \approx 2$,¹³ and equating m with the bare electron mass, we obtain the maximum $n_M \approx 2 \times 10^{17} \text{ cm}^{-3}$ ($n_M \approx 4 \times 10^{-5}$ per unit cell) corresponding to $\Delta T/T \approx 70\%$. From this, we can get rough estimates of trapping and quenching probabilities.

From the temporal dependence of PIA on P and I (see Fig. 3), it follows that both generation and quenching of PIA depend on the dose. Taking into account that $\alpha(3.1 \text{ eV}) \approx 0.5 \text{ cm}^{-1}$,^{1,6} it follows from the data presented in Fig. 2 that only one carrier in about 40 electron-hole pairs created via absorption of visible photons gets trapped. On the other hand, it takes about 100 absorbed NIR photons to quench one of the trapped carriers. In other words, while the initial trapping probability is quite low (of the order of a few percent), when the trapped carriers are excited by absorption of IR (or visible) photons, the retrapping probability is very high ($\approx 99\%$). Once an electron is trapped, it is not easy to untrap it.

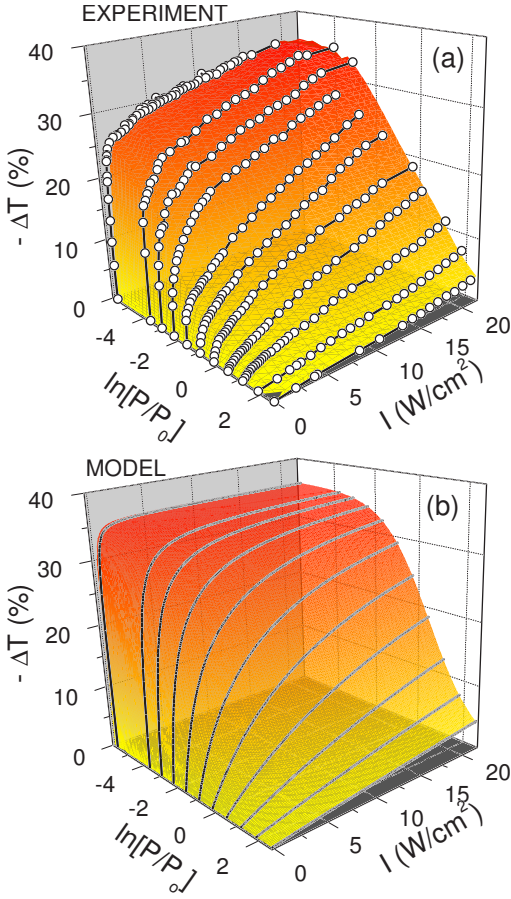


FIG. 5. (Color online) (a) Dependence of $\Delta T/T(0.7 \text{ eV})$ on I and P at 4 K; the latter is shown on a logarithmic scale with $P_0 = 24 \text{ mW/cm}^2$. (b) The same calculated using a solution of a simple three-level model, given by Eq. (2).

C. Nonlinear dependence of photoinduced absorption on the excitation and near-infrared probe fluence

From Fig. 3(a), it follows that the change in transmission ΔT when both the visible photoexcitation and the NIR probe beams are incident on the sample and the quasiequilibrium state is reached depends strongly on P . Studies of the dependence of ΔT on both I and P can therefore help us elucidate the nature of the observed PIA. We have studied the dependence of PIA on the intensity of illumination by varying P and I over 4 and 3 orders of magnitude, respectively. The magnitude of the effect, i.e., $\Delta T/T$, depends on I and P in a complicated, nonlinear way, which is illustrated in Fig. 5(a). Qualitatively, $-\Delta T/T$ initially increases rapidly with I , but the slope decreases and practically saturates at some high fluence. However, the I dependence is strongly affected by P ; for fixed I , $\Delta T/T$ drops very fast as P is increased.

The simplest model that gives a reasonable fit to the data is a three-level scheme with the following key rate equation:¹⁴

$$dn_M/dt = aI - bn_M - cIn_M - dPn_M. \quad (1)$$

Here, n_M is the number density of photogenerated in-gap carriers that give rise to PIA. The first term on the right-hand

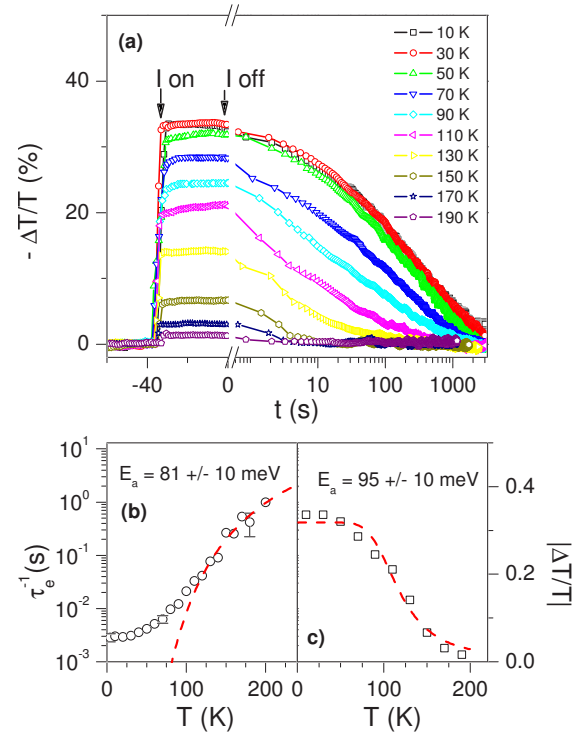


FIG. 6. (Color online) (a) Evolution of $-\Delta T/T(0.7 \text{ eV})$ with time at different temperatures ($I=10 \text{ W/cm}^2$ and $P=1.5 \text{ mW/cm}^2$). (b) Dependence of the effective recombination rate τ_e^{-1} on temperature. The dashed line is a fit to Arrhenius law, $\tau_e^{-1} = b_0 \exp(-E_a/k_B T)$, with $E_a = 81 \pm 10 \text{ meV}$ and $b_0 \approx 100 \text{ s}^{-1}$. (c) The evolution of PIA amplitude with temperature fit using Eq. (2) with $b = b_0 \exp(-E_a/k_B T)$. The extracted value of activation energy is $E_a = 95 \pm 10 \text{ meV}$.

side represents pumping into the in-gap level by absorption of visible light and subsequent trapping of electrons or holes at some trapping centers, where a is proportional to the product of the density of trapping centers and the trapping probability. The third and the fourth terms correspond to quenching of the in-gap level by absorption of visible (pump) and NIR (probe) photons, respectively. The second term corresponds to the intrinsic relaxation of the in-gap state where a single relaxation channel is assumed for simplicity.

To compare our experimental data to the above model, it is convenient to express I and P in number of incoming photons per unit cell per second. Figure 5(b) presents the fit of $\Delta T(I, P)$ data plotted in panel (a) with the solution of Eq. (1) in quasiequilibrium ($dn_M/dt=0$):

$$n_M = aI(b + cI + dP)^{-1}. \quad (2)$$

Clearly, Eq. (1) provides a reasonably detailed description of the observed PIA dynamics. At low T , the intrinsic recombination rate b is very small and can be neglected ($b=0$). From the fit, we can determine the ratio a/c to be of the order of $a/c \approx 10^{-5} \text{ unit cell vol}^{-1}$. It depends, however, on the excitation photon energy and varies also from sample to sample (a is proportional to the density of trapping centers, which depends on the annealing conditions). More importantly, it

follows that $c \approx d$ [for the simulation in Fig. 5(b), we have chosen $c=d=10$ unit cell vol]. This implies that NIR and visible light contribute equally to quenching of PIA. The strongly nonlinear dependence of PIA on I and P comes from the last two terms in Eq. (1), i.e., from self-quenching by photoexcitation I and quenching by P .

The constants b , c , and d can also be extracted directly from the dynamics data presented in Figs. 3 and 4. From the dependence of rise time on I [Fig. 4(b)], one obtains $c = 50$ unit cell vol, and from the P dependence of the decay dynamics [inset of Fig. 3(b)], it follows that $b = 4 \times 10^{-4} \text{ s}^{-1}$ and $d = 30$ unit cell vol. The good agreement between the parameters extracted from the two complementary data sets supports the interpretation.

D. Temperature dependence of the relaxation dynamics

Figure 6 presents the temporal evolution of the PIA peak in the range between 10 and 190 K. While at $T < 50$ K both quasiequilibrium PIA and relaxation time show only weak T dependence, at higher T , both rapidly decrease. This behavior is consistent with the observation that at low T , the relaxation is essentially governed by the NIR quenching mechanism, while at higher T , the dominant contribution is from the intrinsic relaxation represented by the second term in Eq. (1). The latter is supported by the fact that above 100 K, the relaxation of PIA is found to be independent of P over 3 orders of magnitude in P (data not shown).

To study the evolution of the recovery dynamics with T , we fit the decay dynamics with $A \exp[-(t/\tau_e)^p]$ and the stretching parameter fixed at $p=0.5$. As shown in Fig. 6(b), τ_e^{-1} changes by 2 orders of magnitude between 100 and 190 K and can be well fitted by the thermally activated (Arrhenius) law, $\tau_e^{-1} \sim b_0 \exp(-E_a/k_B T)$, with the activation energy $E_a \approx 80$ meV. Strong T dependence of b is expected to influence also the quasiequilibrium PIA. Indeed, assuming that rates a , c , and d are T independent, we can fit the T dependence of the amplitude with Eq. (2) quite successfully [Fig. 6(c)]. With $b = b_0 \exp(-E_a/k_B T)$, we obtain comparable value for E_a (95 meV), supporting the idea that the T dependence of PIA transient essentially comes from the T dependence of the intrinsic relaxation rate.

III. DISCUSSION

We have shown that only a small fraction of the absorbed IR photons (about 10^{-2}) contribute to quenching of the PIA. This implies strong geminate recombination, indicative of a small escape radius and low mobility (or a large effective mass) of photoexcited electrons and holes. If trapped electron is excited by absorbing an IR photon, it is likely to rapidly drop back to the same “trap” which involves a local dynamic distortion of the crystal and takes time to relax. Only rarely, because of thermal or quantum fluctuations, will an excited electron escape, drift away, and find a hole to collide with and recombine. Intrinsic in-gap states could be long lived because of the existence of a barrier for recombination; if either electrons or holes are localized, they cause local lattice distortion, and this can cause the interaction be-

tween opposite charges to change sign and become repulsive at short range. The strong T dependence may come from the increase in mobility and/or in the attempt frequency (to traverse the barrier and recombine) or from increased number of thermally activated phonons that help electrons and/or holes to tunnel through and recombine. A strong geminate recombination of electron-hole pairs is also supported by the low trapping probability for carriers excited by absorption of visible photons.

Such experimental observations have been frequently (in particular, in the literature on high- T_c superconductors⁸) hailed as fingerprints of formation of small polarons or bipolarons. Note that the shape of PIA in LaSrAlO₄ can be fitted almost perfectly [see Fig. 1(a)] to Poisson-distribution-like formula with $\hbar\omega_0 \approx 70$ meV and a mean number of quanta $\eta \approx 10$. The shape is exactly as predicted for optical absorption due to electrons (or holes) self-trapped by strong coupling to optical phonons.^{15,16} Far-IR optical spectroscopy shows the existence of dipole active modes in the 55–80 meV range at the Brillouin zone center.¹³ Indeed, quite similar PI features have been observed, e.g., in SrTiO₃ where photoexcited electrons self-trap form small polarons and bind with holes into long-lived self-trapped excitons about 0.7 eV below the conduction band.¹⁷ Moreover, chemical doping or photodoping is believed to create small polarons and gives rise to similar mid-IR absorption peaks in other oxides such as tungstates, tantalates, vanadates, nickelates, cobaltates, ruthenates, etc. However, the fact that we do not observe such visible light induced PIA features in pristine LSAO crystals and only see them after the crystals are annealed in a strongly reducing atmosphere clearly ties PIA to the existence of O vacancies in LSAO. Given the fact that oxygen defects are present in many of oxides,⁹ it is quite feasible that their presence affect their MIR properties in many of these compounds. In this paper, we show the way how to elucidate these questions. In fact, it was reported just recently that the high frequency peak in the PIA in La₂CuO₄ stems from surface carriers¹⁸ in contrast to previous reports.⁸

IV. CONCLUSIONS

In conclusion, we have studied the changes in the NIR optical properties in series of LaSrAlO₄ samples induced by absorption of visible sub-band-gap photons. Strong photoinduced absorption centered at ≈ 0.7 eV was observed in samples annealed in a reduction atmosphere associated with the treatment induced oxygen vacancies. The magnitude of the PIA varied from sample to sample, while its spectral shape being independent of sample and temperature. The effect was found to depend strongly on both the excitation intensity as well as on the intensity of the probe which was quenching the PIA. The results obtained by varying excitation and probe intensities over several orders in magnitude enabled us to construct a simple three-level model that successfully describes the data, enabling us to extract several material specific parameters.

At low temperatures, the PIA was found to persist for hours in the absence of probe. From the dependence of the dynamics on excitation and probe intensities, we were able

to determine the trapping and quenching probabilities. The low trapping and quenching probabilities together with the fact that strong PIA was observed in oxygen pure samples suggest that photoexcited carriers self-trap in the vicinity of oxygen vacancies. The trapping induces local lattice distortions which take time to relax. Therefore, the trapped carriers excited by absorption of NIR photon get efficiently retrapped at low temperatures with the quenching probability being very low. Upon increasing the temperature, the relaxation rate is increased, showing activated temperature dependence with the activation energy of about 90 meV. From the systematics of the PIA amplitude and associated dynamics as a function of excitation intensity, NIR probe intensity, and temperature, we conclude that the origin of strong PIA in

LaSrAlO₄ is in self-trapping of photoexcited carriers in the vicinity of oxygen vacancies. Note that the latter are indeed ubiquitous to transition-metal oxides, and hence one might question whether some of the reported small polaron behavior were, in fact, due to O vacancies. The present paper shows a simple way to answer this question.

ACKNOWLEDGMENTS

This work was supported by NATO EAPRIG.98142, CINT-U2006A161, and US DOE Contract No. MA-509-MACA. J.D. acknowledges discussions with V. Kabanov, M. Zgonik, and A. S. Alexandrov.

-
- ¹A. Gloubokov, R. Jablonski, W. Ryba-Romanowski, J. Sass, A. Pajaczkowska, R. Uecker, and P. Reiche, *J. Cryst. Growth* **147**, 123 (1995).
- ²R. Brown, V. Pendrick, D. Kalokitis, and B. H. T. Chai, *Appl. Phys. Lett.* **57**, 1351 (1990).
- ³I. Bozovic, G. Logvenov, I. Belca, B. Narimbetov, and I. Sveklo, *Phys. Rev. Lett.* **89**, 107001 (2002); I. Bozovic, G. Logvenov, M. A. J. Verhoeven, P. Caputo, E. Goldobin, and M. R. Beasley, *ibid.* **93**, 157002 (2004); I. Bozovic, G. Logvenov, M. A. J. Verhoeven, P. Caputo, E. Goldobin, and T. H. Geballe, *Nature (London)* **873**, 422 (2003).
- ⁴W. Ryba-Romanowski, S. Golab, G. Dominiakdzik, A. Pajaczkowska, and M. Berkowski, *J. Phys. IV* **4**, C4-561 (1994); W. Ryba-Romanowski, S. Golab, W. A. Pisarski, G. DominiakDzik, M. Berkowski, and A. Pajaczkowska, *Int. J. Electron.* **81**, 457 (1996).
- ⁵G. Ross, G. Montemezzani, P. Bernasconi, M. Zgonik, and P. Gunter, *J. Appl. Phys.* **79**, 3665 (1996).
- ⁶M. Gao, R. Pankrath, S. Kapphan, and V. Vikhnin, *Appl. Phys. B: Lasers Opt.* **68**, 849 (1999).
- ⁷T. Mertelj, D. Kuscer, M. Kosec, and D. Mihailovic, *Phys. Rev. B* **61**, 15102 (2000).
- ⁸G. Yu and A. J. Heeger, *Int. J. Mod. Phys. B* **7**, 3751 (1993); D. Mihailovic, C. M. Foster, K. Voss, and A. J. Heeger, *Phys. Rev. B* **42**, 7989 (1990); J. D. Perkins, R. J. Birgeneau, J. M. Graybeal, M. A. Kastner, and D. S. Kleinberg, *ibid.* **58**, 9390 (1998); Y. H. Kim, S.-W. Cheong, and Z. Fisk, *Phys. Rev. Lett.* **67**, 2227 (1991).
- ⁹A. Gilabert, A. Hoffmann, M. G. Medici, and I. K. Schuller, *J. Supercond.* **13**, 1 (2000); J. Federici and D. M. Bubb, *ibid.* **14**, 331 (2001).
- ¹⁰W. Ryba-Romanowski, S. Golab, I. Sokolska, W. A. Pisarski, G. Dominiak-Dzik, A. Pajaczkowska, and M. Berkowski, *J. Alloys Compd.* **217**, 263 (1995).
- ¹¹J. Hora, K. Navratil, J. Humlicek, and M. Berkowski, *Phys. Status Solidi B* **195**, 625 (1996).
- ¹²C. P. Lindsey and G. D. Patterson, *J. Chem. Phys.* **73**, 3348 (1980).
- ¹³G. X. Chen, Y. J. Ge, C. Z. Bi, X. G. Qiu, and B. R. Zhao, *J. Appl. Phys.* **95**, 3417 (2004); J. Humlicek, R. Henn, and M. Cardona, *Phys. Rev. B* **61**, 14554 (2000).
- ¹⁴Here, it is assumed that the density of trapping centers is large compared to the density of photogenerated carriers.
- ¹⁵K. Huang and A. Rhys, *Proc. R. Soc. London, Ser. A* **204**, 406 (1950).
- ¹⁶H. G. Reik, *Z. Phys.* **203**, 346 (1967).
- ¹⁷R. Leonelli and J. L. Brebner, *Phys. Rev. B* **33**, 8649 (1986).
- ¹⁸R. V. Yusupov, K. Conder, T. Mertelj, D. Mihailovic, K. A. Müller, and H. Keller, *Eur. Phys. J. B* **54**, 465 (2007); R. V. Yusupov, V. V. Kabanov, D. Mihailovic, K. Conder, K. A. Müller, and H. Keller, *Phys. Rev. B* **76**, 024428 (2007).